Targeting STAT3 by HO3867 induces apoptosis in ovarian clear cell carcinoma

Kristin Bixel[1], Uksha Saini[1], Hemant Kumar Bid[2], John Fowler[1], Maria Riley[1], Ross Wanner[1], Kalpana Deepa Priya Dorayappan[1], Sneha Rajendran[1], Ikuo Konishi[3], Noriomi Matsumura[3], David E. Cohn[1] and Karuppaiyah Selvendiran[1]

[1]Division of Gynecologic Oncology, Comprehensive Cancer Center, The Ohio State University Wexner Medical Center, Columbus, OH.

[2]Cancer Therapeutics, Life Sciences Institute University of Michigan campus, Ann Arbor, MI

[3]Division of GYN/ONC, Kyoto University Graduate School of Medicine, Kyoto, Japan

[#]Corresponding Authors:

Karuppaiyah Selvendiran, Ph.D,
Division of Gynecologic Oncology,
The Ohio State University Wexner Medical Center,
Columbus, OH 43210.
Phone: 614-685-4183
E-mail: selvendiran.karuppaiyah@osumc.edu

Novelty and Impact: Ovarian clear cell carcinoma (OCCC) is an aggressive form of ovarian cancer and accounts for 5–25% of epithelial ovarian cancers. Worse treatment outcomes for OCCC have been attributed to its relative chemoresistance. The overall clinical response in chemotherapy-treated patients with recurrent OCCC is only 25-40%. Therefore, the investigation and development of new compounds is necessary to overcome the high rates of drug resistance in OCCC. Our results indicate high levels of expression of phosphorylated STAT3 (pSTAT3Tyr705 and Ser727) in ovarian clear cell carcinoma (OCCC), which may prove to be an important chemo-resistant pathway for OCCC.

Abstract

Advanced ovarian clear cell carcinoma (OCCC) carries a very poor prognosis in large part secondary to the extremely high rate of resistance to standard platinum and taxane chemotherapy. STAT3 expression and activation has been shown to regulate tumor progression in various human cancers, though has not been well studied in OCCC. Preliminary work in our lab has demonstrated constitutive activation of STAT3 (pSTAT3Tyr705 or pSTAT3727) in OCCC cell lines as well as human OCCC tumor tissue samples. Significantly, pSTAT3 is expressed in the absence of other forms of activated STAT (pSTAT1, 2, 6). Therefore, this work was planned to investigate the role of STAT3 and examine the efficacy of a novel anti-cancer compound -HO-3867, which is an inhibitor of STAT3, using known OCCC cell lines. Results demonstrate that treatment with HO-3867 decreased expression of pSTAT3 Tyr705 as well pSTAT3 Ser727, while total STAT3 remained constant. STAT3 overexpression increased the migration capability in OVTOKO cells *in vitro* and led to an increased tumor size when injected *in vivo*. The inhibitory effect of HO-3867 on cell proliferation and cell survival was accompanied by increased apoptosis, within 24 h post treatment. Treatment with HO-3867 resulted in a decrease in Bcl-2 and increase of cleavage of caspase 3, caspase 7, and PARP, confirming induction of apoptosis after treatment with HO-3867. In addition, HO-3867 significantly inhibited formation of HUVEC cells capillary-like structures and invasion at both 5 and 10μM concentrations. STAT3 expression plays an important role in the spread of OCCC *in vitro* as well as *in vivo*. Thus, we can exploit the STAT3 pathway for targeted drug therapy. Inhibition of pSTAT3 using HO-3867in OCCC cell lines appears to be a promising therapy. This is of utmost importance given the poor response of OCCC to standard chemotherapy regimens.

Key words: Ovarian clear cell carcinoma, STAT3, HO-3867, curcumin analog, angiogenesis

Introduction

Ovarian clear cell carcinoma (OCCC) accounts for approximately 5 to 25% of epithelial ovarian cancers with varying incidence by population[1-3]. Though rare, it presents a unique treatment challenge. While OCCC tends to present at earlier stages, women with advanced disease have a poor prognosis compared with other epithelial ovarian cancer (EOC) subtypes[3-5]. This is illustrated by a meta-analysis of multiple clinical trials of advanced-stage EOC that noted a median overall survival of 21.3 months for women with OCCC, compared to 40.8 months for those with high grade serous ovarian cancer (HGSOC)[5]. It has been hypothesized that the discrepancy in outcomes may be at least in part secondary to tumor resistance to chemotherapy. While platinum-based chemotherapy is standard first-line treatment for EOC, OCCC does not respond well to the regimen. In a multi-center retrospective study of patients with stage III/IV OCCC with measurable disease after surgery, response to platinum-based chemotherapy was 11.1%, as compared to 72.5% in patients with HGSOC [4]. Another analysis of data from multiple clinical trials for advanced ovarian cancer found that overall response rates were 45% for OCCC versus 81% for HGSOC[6, 7].

While the relative chemoresistance of OCCC is felt to portend a worse prognosis, the precise mechanism of resistance remains unclear. Thus, to improve outcomes for patients diagnosed with OCCC, it is critical to find ways to overcome chemoresistance or identify new targets for therapy. Signal transducer and activator of transcription 3 (STAT3) is a transcription factor that mediates cytokine and growth factor signaling. STAT3 activation contributes to tumorigenesis by promoting cell proliferation, survival, angiogenesis, metastasis, inflammation, and immune evasion [8-11]. STAT3 expression and activation has been shown to regulate tumor progression in various human cancers including HGSOC, though has not been well studied in OCCC. OCCC is characterized by a high rate of ARID1A and PI3K mutations which have been shown to cooperate in animal models to promote OCCC tumor growth through sustained IL-6 overproduction leading to increased activation of STAT3[12]. Additionally, Anglesio et al demonstrated overexpression of IL6-STAT3-HIF pathway in OCCC[13]. These findings support further investigation into STAT3 as a potential therapeutic target in OCCC.

We have previously shown that activation of STAT3 is necessary for HGSOC tumor progression/metastasis and targeting STAT3 with HO-3867 (a member of a novel class of anti-

cancer drugs, diarylipenylpiperiden-4-ones (DAP's) significantly suppressed tumor growth and metastasis[10, 14-16]. Therefore, this study was designed i) to investigate and establish the role of STAT3 in OCCC progression in OCCC cells and human OCCC patient tissue samples ii) to examine the efficacy of our STAT3 inhibitor, HO-3867 *in vitro* and *in vivo* using the orthotopic tumor model.

Material and Methods

Culture of OCCC cells: The OCCC cell lines OVTOKO, JHOC, OVISE and ES2 were a kind gift from Ikuo Konishi, Kyoto Medical University, Japan. The cells were cultured in T75 flasks in RPMI medium supplemented with FBS (10%) and Penicillin/ streptomycin (1%).

Immunocytochemistry: Cells in RPMI medium were seeded onto sterile glass coverslips in 6-well plates with an average population of 50,000 cells/well. After 24 hours of culture, the cells were washed, fixed, and incubated with primary antibody according to a previously described protocol.

STAT3 overexpression/knockdown experiments: For downregulation of STAT3 in OVTOKO cells, a lentiviral system with a set of different short hairpin RNAs (shRNA) was used (Stat3 shRNA (h) Lentiviral Particles, Santa Cruz Biotechnology, Texas, USA) using Dharmafect Transfection Reagent (GE, Lafayette, CO) in OVTOKO cells. For STAT3 overexpression, we used EF.STAT3C.UbC.GFP, which was a gift from Linzhao Cheng (Addgene plasmid#24983), transfected into OVTOKO cells using Dharmafect Transfection Reagent (GE, Lafayette, CO).

Immunoblot analysis: Cells in were treated with HO-3867 (5 μM or 10 μM) for 24 hours. Following treatment, the cell lysates were prepared in non-denaturing lysis buffer as previously described [17].

Cell migration Assay: Cell migration assays were performed on both treated and non-treated cells using a wound-healing method [18].

RNA isolation and Reverse Transcription PCR (RT PCR): OVTOKO cells were counted and plated in equal numbers in petridishes. The petridishes were treated with HO-3867 at 5 and 10μM concentrations, with at least 3 plates per treatment. At 24 hours post treatment, the cells were collected and stored in the -80°C until further use. Total RNA was isolated using the RNeasy Mini Kit (Qiagen, Valencia, CA). RNA samples with an optical density A260/A280

ratio between 1.8 and 2.1 were used. RT-PCR was then performed using the Transcriptor First Strand Complementary DNA (cDNA) Synthesis Kit (Roche Applied Science) to synthesis cDNA. RT-PCR was performed with 1mg of RNA template. The reaction was carried out using the Veriti Thermal Cycler (Applied Biosystems, Carlsbad, CA) and random hexamer primers.

Quantitative Real Time PCR (qPCR): The genes studied for their relative genetic expression patterns are provided in Table 1. LightCycler 480 SYBR Green I Master Mix (Roche Applied Science) was used to analyze 100 ng of cDNA from each experimental condition along with their respective primers (Table I). qRT-PCR was performed using the Light Cycler 480 System (Roche Applied Science). Each sample was normalized to the control gene glyceraldehyde 3-phosphate dehydrogenase (GAPDH.

STAT3 DNA-binding assays: After treatment with HO3867 for 24 hours, a nuclear extract kit (Clontech Inc., Mountain View, CA) was used to prepare cell nuclear extracts following the manufacturer's protocol. Nuclear extracts were analyzed for STAT3 DNA binding activity using the TransFactor Universal STAT3-specific kits (Clontech Inc., Mountain View, CA) with an ELISA-based method.

Ubiquitin assay: To trace the ubiquitinated proteins in the cell lysates, agarose beads coated with domains having affinity to ubiquitin were incubated in the lysates at 4°C for 2 hours. After washing the beads, the ubiquitinated proteins were subjected to immunoblot for pSTAT3 and blotted by the ubiquitin antibody[19].

Evaluate the bio-absorption of DAPs in ovarian cancer cells using EPR: Our previous study showed that cellular uptake of HO-3867 was significantly greater than curcumin [20]. We evaluated the bio absorption of HO-3867 compounds in ES2 and OVTOKO cells after 1, 3 , and 6 hrs post treatment, using EPR, as previously described [21].

Development of orthotopic tumor model

STAT3 overexpression OCC cells ($3 \times 10^{*6}$ cells in 100 μL of PBS) were injected into the ovarian bursa of 6-week-old BALB/c nude mice from the OSU Transgenic mice core lab. In vivo MRI imaging was done periodically to check upon the tumor growth. After sacrifice, the tumor weight and volume was measured.

Statistical Analysis

Data are presented as mean±1 standard deviation

RESULTS

Validate the expression of STAT3 in OCCC cell lines and human patient tissue samples

We received 7 OCCC tissue samples from consented patients with OCCC at our institution and analyzed the expression of pSTAT3 Tyr705, pSTAT3 Ser727 and total STAT3. Five out of 7 samples showed moderate to high expression of pSTAT3Tyr705 on Western Blot (**Fig. 1A**). Expression was tested in OCCC cell lines (JHOC and OVTOKO) that were gifted by Dr. Konishi at Kyoto University for the current study. The studied cell lines showed moderate to high expression of pSTAT3 Tyr705, Ser727 and total STAT3, when analyzed by western blot (**Fig. 1B**). pSTAT3 Tyr705 showed high expressions in all tested cell lines (Fig. 1B). OVTOKO cells (90-95%) showed pSTAT3 Tyr705 localized in the nucleus as well as the cytoplasm while pSTAT3 Ser727 was mostly found in the cytoplasm of OVTOKO cells (**Fig. 1C**).

Effect of STAT3 overexpression or knockdown in ovarian clear cell carcinoma cells *in vitro* as well as *in vivo.*

In our previous studies with HGSOC, we found that the knockdown of STAT3 causes reduction in tumor growth and metastases *in vivo*[10]. Based on this finding, we considered it imperative to determine if STAT3 plays a role in cell proliferation, migration, and survival OCCC cell lines as well. Therefore, we developed OVTOKO STAT3 overexpression (STAT3 OE) cells by transfecting OVTOKO cells with a plasmid construct constitutively expressing pSTAT3 Tyr705. **Fig. 2A** shows the western blot expression of pSTAT3 Tyr705 in 4 of the tested OE clones. We found that clone O6 showed the highest expression of pSTAT3 Tyr705 so we moved forward with this clone for our future studies. Additionally we used siRNA for STAT3 to knockdown STAT3 from the OVTOKO cells, which was confirmed by western blot (**Fig. 2B & C**). Since an increased STAT3 expression is known to cause extensive migration as well as invasion[10, 22] , we analyzed the changes in the wound closure behavior of the cells. To confirm this, we performed a wound healing assay, where a monolayer of cells growing on a petri dish were scratched uniformly and observed at 24 hours for their ability to repair the damaged area for the control OVTOKO cells, OVTOKO STAT3 OE as well as OVTOKO STAT3 KO cells. The control OVTOKO and OVTOKO STAT3 OE cells migrated at about the same rate in the first 24 hours.

However, OVTOKO STAT3 KO cells migrated to approximately 20 to 30% of the wounded area (**Fig. 2D & E**).

This was further confirmed at the mRNA level using real time quantitative PCR to check the relative expression of genes related to angiogenesis, cell survival and cell proliferation. The relative mRNA expression of STAT3 was highest in OVTOKO STAT3 OE cells followed by the control OVTOKO cells and OVTOKO STAT3 KO cells (**Fig. 2F**). The STAT3 target genes like Survivin, VEGF, c-myc and BCl2 were highest in the OVTOKO STAT3 OE cells and least in the OVTOKO STAT3 KO cells (**Fig. 2F**). Taken together, these results suggest that deleting STAT3 inhibits the expression of a number of genes responsible for cell survival, proliferation and angiogenesis. These findings were further evaluated *in vivo*. The OVTOKO control and OVTOKO STAT3 OE cells were injected into the right ovarian bursal cavity of nude mice (**Fig. 2G**). It is noteworthy that the mice injected with control OVTOKO cells failed to develop any primary tumor in the first 5 weeks post inoculation. However, the mice injected with OVTOKO STAT3 OE cells developed significantly large tumors as demonstrated in **Fig.2H**. No metastases were observed in any of the cases. These results add support to the role of STAT3 in OCCC tumor development and growth, and its ability to regulate the expression of different genes involved in survival and proliferation.

HO-3867 targets on STAT3 and its associated genes in OCCC cells

We used OVTOKO and JHOC cell lines to test the therapeutic efficacy of our previously developed novel DAP compound on OCCC cell lines. We treated the OVTOKO and JHOC with 2 different concentrations (5 and 10μM) of HO-3867. Western blot expression in **Fig. 3A** clearly shows that the expression levels of both pSTAT Tyr705 and pSTAT Ser727 drastically decreases even in the lowest dose of 5 μM and is almost non-existent in the higher dose of 10μM for both the tested OCCC cell lines (**Fig. 3B**). To determine whether HO-3867 inhibited pSTAT3 DNA binding activity, OVTOKO and JHOC cells were treated with 10μM of HO- 3867, and samples were subjected to ELISA assay. HO-3867 compound inhibited STAT3 DNA binding activity in both cells when compared with control **(Fig. 3C)**. Further, the STAT3 regulated genes like JAK1, Tyk2 and CDK5 also showed a diminished expression post treatment with HO-3867 for both the tested OCCC cell lines. MCL1, BCl2, Cyclin D2 and c-myc were also decreased post

HO-3867 treatment for both JHOC and OVTOKO cells (**Fig. 3D&E**). This demonstrates that HO-3867 effectively targets STAT3 and its associated genes in OCCC cells. We sought to confirm these findings at the level of relative mRNA expression using qRT-PCR. The RNA obtained from the treated OVTOKO cells was converted to cDNA and subjected to real time PCR using the gene specific primers for STAT3, JAK1, BCl2, c-myc and cyclin D1. We found that mRNA expression for STAT3 and JAK1 was decreased post treatment with HO-3867 at both the doses of 5 & 10uM. However, the expression levels of BCl2, c-myc and cyclin D1 were not significantly decreased after treatment with HO-3867 (**Fig. 3F**).

Ubiquitination is the first step of the ubiquitin-proteasome pathway that regulates cells for their homeostatic functions and is an enzymatic, protein post-translational modification process in which ubiquitin is transferred to a target protein substrate by a set of three ubiquitin enzymes[23-25]. Given the importance of this process, it is plausible that HO-3867 has a function to regulate the ubiquitination. Therefore, we examined the ubiquitination status of the OVTOKO cells post treatment with HO-3867 and observed an enhanced degradation in both OVTOKO and JHOC cells post treatment for both the concentrations. Further, the degradation was concentration specific and increased with the increasing dosage of HO-3867 (**Fig. 3G**).

HO-3867 inhibits cell survival and increase the caspase cascade pathway

To evaluate the effect of HO-3867 on OCCC survival, we treated cells with different concentrations (1, 2.5, 5, 10 and 20 uM) of HO-3867 at time points (24 and 48 h). Cell viability was measured by MTT assay and cell count. The proliferation and survival of OCCC cells were inhibited by HO-3867 in a dose-dependent manner (**Fig. 4A**). Caspases are aspartic acid-specific proteases and are the major effectors of apoptosis. Therefore, in order to confirm if the activity of HO-3867 also activates the caspase cascade, we performed western blot on OVTOKO, ES-2, OVISE and JHOC cells and found that PARP, cleaved caspase 3 and cleaved caspase 9 were all upregulated post treatment with HO-3867 (**Fig. 4B**). As an additional proof of concept experiment, we further studied the caspases in ES2 and OVISE cells and found that the higher dose of 20 μM was able to activate cleaved caspase 3 and cleaved caspase 7 and PARP was activated even by the lower dose of 10 μM (Fig. 4B). This was further confirmed by Annexin V staining assays using a flow cytometer. It is known that in early stages of apoptosis, the plasma

membrane excludes viability dyes such as propidium iodide (PI) and display only Annexin V staining. We observed an increase in the percent of Annexin V positive cells post treatment with 30 to 51% of apoptotic cells post treatment as compared to 5 to 10 % cells undergoing apoptosis in the untreated cells (**Fig. 4C&D**). The HO-3867-treated STAT3-overexpressing cells showed increase cell proliferation and decrease apoptotic proteins, in comparison with HO-3867 alone treated cells (**Fig. 4E & F**), suggesting that HO-3867 might target, at least in part, STAT3 in OCCC. EPR spectrum obtained from ovarian clear cell carcinma showing the presence on HO-3867 in the oxidized (nitroxide) form. HO-3867 levels in the cells samples were determined using EPR, clear, triplet signals indicating the presence of the –NO_ radical (nitroxide) form of HO-3867 were obtained from both cell lines and quantified (**Fig. 4G & H**).

Effect of HO3867 on human endothelial (HUVEC) cells

In the ovarian clear cell tumor microenvironment, tumor cells secrete VEGF and other angiogenic factors that promote the growth and assembly of neighboring endothelial cells. Since HO-3867 can block secretion of important angiogenic proteins, we next examined if HO3867 treatment suppresses the growth and differentiation of human umbilical vein endothelial cells (HUVEC) in response to treatment with VEGF. HO-3867 significantly inhibited formation of capillary-like structures at both 5 and 10μM concentrations (**Fig. 5A**), indicating that signaling through STAT3 is necessary for VEGF-stimulated proliferation and tube formation of these endothelial cells. A 3D angiogenesis model utilizing VEGF stimulated HUVEC spheroids embedded in a collagen matrix recapitulates the inhibition of tube-like formation by HO3867 seen in the two-dimensional model. After successful stimulation, new blood vessels sprouted into the collagen matrix within 2-3 days and were quantified in the presence and absence of HO3867. Fewer number and shorter length of the sprouts demonstrates the anti-angiogenic activity of HO3867 in comparison to the control group (**Fig. 5B**). HO3867 treatment also significantly blocked the invasion of VEGF-stimulated HUVECs through a Boyden chamber (**Fig. 5C**).

Cytosolic STAT3 is known to be a co-regulator of F-actin fiber [26] and microtubule [27] formation. The disruption of lamellipodia formation and microtubule breakdown at the trailing edge may explain the drastically reduced invasion of HUVEC cells. In order to confirm this, HUVEC cultures were treated with VEGF alone, VEGF plus DMSO (drug vehicle) or VEGF

with HO-3867 for 18 hrs followed by staining for F-actin and b-tubulin. (**Fig. 5D**). Thin, uniform fibers spanning the length of the cells were characteristic of the F-actin in the control and VEGF-treated cultures, with greater localization at the peripheral lamellipodia and intercellular junctions. The microtubules extended to the periphery of the cells forming a dense lattice that emanated from the center of the cells. However, in STAT3 inhibited cultures, the cells displayed a condensed and rounded morphology. The actin had condensed into fewer fibers, and most strikingly, was completely absent from the leading edges of the cells (white arrows, **Fig. 5D**). The microtubule structures were additionally affected by the HO-3867 treatment. As highlighted by the arrowheads in Figure 5D, tubulin staining still showed that the microtubules emanated from the nuclear region of the HUVEC cells, but at the periphery, they curled over.

Discussion

Our results indicate high levels of expression of phosphorylated STAT3 (pSTAT3Tyr705 and Ser727) in ovarian clear cell carcinoma (OCCC) which may prove to be an important pathway for OCCC cell survival, proliferation, and angiogenesis. Further, this is the first report proving the efficacy of HO-3867, a curcumin analog, in inhibiting OCCC cell survival and proliferation; induction of apoptosis and inhibition of angiogenesis by targeting the activation of STAT3.

Recent studies have identified potential driver genes and aberrant signaling pathways involved in development of OCCC [7, 28, 29]. As described above, ARID1A and PI3K mutations are detected in more than 55% and 30% of OCCC cases respectively[2, 12]. Co-existent ARID1A and PI3K mutations have been shown to promote OCCC tumor growth through overproduction of IL-6 and activation of STAT3 lending STAT3 an attractive target for therapy[12, 13]. Although, the expression of STAT3 oncogene is well known in high grade serous ovarian cancer (HGSOC)[9, 10, 30, 31], moderately little is known about the STAT3 signaling pathways in OCCC; its involvement in chemo-resistance and poor survival or its potential as a therapeutic target. This study identified a) the expression of STAT3 in OCCC patient tissues and cell lines and b) STAT3 expression can up-regulate its target genes such as c-MYC (proliferation), and Bcl-2 (cell survival and anti-apoptotic) thus playing a key role in proliferation and tumor progression of OCCC. Recent studies in renal clear cell carcinoma have associated higher expression of

pSTAT3 with the tumor grade and poor patient survival[32, 33]. It is clearly evident from our study that the expression of STAT3 might affect patient survival in OCCC, and targeting STAT3 using small molecule inhibitors could possibly inhibit OCCC tumor growth and help overcome the chemotherapeutic resistance in OCCC tumors.

We have recently reported four promising DAP compounds which are STAT3 inhibitors-H-4073, HO-3867, H-4318 and HO-4200[15, 16, 34]. HO-3867 demonstrate high cytotoxicity towards human ovarian cancer cells, including those known to be chemo-resistant, under both *in vitro* and *in vivo* conditions [14]. We have selected one of our best DAP compound STAT3 inhibitor-HO-3867, based on the STAT3 DNA binding activity and selective cytotoxicity in cancer cells rather than normal epithelial cells, for the current study. HO-3867 significantly inhibits pSTAT3 in OCCC cells, through the upstream pathways of STAT3 such as JAK and TYK2. In addition, the current study showed an enhanced poly-ubiquitination of pSTAT3 by HO-3867 treatment in OCCC. These results suggest that in OCCC, HO-3867 targets STAT3 through dual pathways—the ubiquitin-dependent degradation of pSTAT3 and the inhibition of upstream regulators of pSTAT3, such as JAK1 and TYK2, eventually inhibiting cell proliferation and inducing apoptosis via modulating its target genes (Cyclin D1 and Bcl-2).

Targeting angiogenesis and VEGF is another therapeutic approach used in treatment of several solid tumors, OCCC included [13, 35]. VEGF was reported to be strongly expressed in OCCC cells and patient samples, both in early- and advanced-stage disease. High levels of VEGF expression are additionally associated with shorter survival than those with lower levels of VEGF expression in OCCC[6, 35]. In this study, we document direct effect of HO-3867, by suppressing HUVEC cell migration/ invasion, tube formation of endothelial cells and affecting the microtubule structures. This proves that STAT3 signaling closely governs these processes and affect STAT3 downregulated protein - VEGF in OCCC. Further, clinical evidence showed that sunitinib, a potent VEGF inhibitor, is more responsive in the treatment of clear cell carcinoma patients than serous tumors[6, 36, 37].

In conclusion, we demonstrate that pSTAT3 expression is highly elevated in OCCC tumors and is a potential therapeutic target for this disease. Our small molecule STAT3 inhibitor of HO-3867 efficiently inhibits pSTAT3 and its target proteins, thereby impeding cell

proliferation, angiogenesis and cytotoxicity in OCCC and seems promising in the future treatment of ovarian clear cell carcinoma.

Acknowledgments

We have greatly acknowledged to Pushpa Lata, Ph.D for her in vitro angiogenesis works in HUVEC cells. This work was funded by Ohio State University Drug Development Institute (OSU-DDI) and NCI RO1-CA176078 grant (K.S and D.E.C).

Figure Legends

Fig. 1: Validation of the expression of STAT3 in OCCC cell lines and human patient tissue samples. **A:** Western blot for Human OCCC tumor samples obtained from 7 consented OCCC patients. The extracted proteins blotted on a PVDF membrane were probed for pSTAT3 Tyr705 (topmost), pSTAT3 Ser727 (middle lane), total STAT3 (lower lane). All the samples show a medium to high pSTAT3 Tyr705 expression except for patient no. 3 and 7. All the patients showed pSTAT3 Ser727 and total STAT3 expression. **B:** Western blot results for human OCCC cell lines-JHOC (J), and OVTOKO (OV). Both cell lines showed a high range of expression of pSTAT3 Tyr705 and pSTAT3 Ser727 (highly elevated in OV) and total STAT3. **C:** Immunocytochemistry (ICC) of OCCC cell line OVTOKO with pSTAT3 Tyr705 (left 2 in the row) which is mostly nuclear and pSTAT3 Ser727 (right 2) which is predominantly cytoplasmic.

Fig. 2: Effect of STAT3 overexpression or knockdown in ovarian clear cell carcinoma cells *in vitro* as well as *in vivo.* **A:** Confirmation of STAT3 overexpression in OVTOKO cells using a Western Blot where N is control OVTOKO, O1, O3, O5 and O6 are overexpression clones 1,3,5 and 6. The bottom panel is β-actin expression as loading controls. In order to create STAT3 overexpression cells, OVTOKO cells were transfected with a vector harboring STAT3 gene or with the empty vector backbone for control. Based on the strongest expression in clone O6, we proceeded with this clone for all our future studies. **B & C:** OVTOKO cells were transfected with STAT3 shRNA and the knockdown was confirmed by western blot analysis and RT-PCR. Knockdown of pSTAT3 705 in OVTOKO cells is clearly evident. **D:** OVTOKO cells with STAT3 overexpression and STAT3 knockdown were subjected to wound healing assays in order to understand the correlation between STAT3 expression level and migration capability in OVTOKO cells. The panel on the left shows the plates at 0 hr after scratch and the panel on the right show the migration pattern after 24 hours. The cells over-expressing STAT3 migrate and close the gap within the first 24 hours (top and middle picture on the right panel) while the STAT3 knockdown cells (bottom left) migrate to fill 65-70% of the scratched area. **E:** The percentage of migration was quantified using Image J software in 0h, 24h compared with STAT3 OE and siRNA experiments; **F:** Real time quantitative PCR was performed for the relative mRNA expression of STAT3 in OVTOKO control, OVTOKO STAT3 OE and OVTOKO

STAT3 Ko cells. The values were calculated using the 2(-Delta Delta C(T)) method and were normalized to the housekeeping gene GAPDH. Each experiment was repeated thrice and each sample had 4 replicates. The horizontal line over the bars indicates that the results are significant with a p value ≤ 0.005**.**RT. RT-qPCR of OVTOKO, OV STAT3 Si and OVTOKO STAT3 OE cells for STAT3 and regulatory genes- survivin, VEGF, c-myc and BCl2. The very high relative mRNA expression was observed in OVTOKO STAT3 OE cells for all the studied genes. **G:** The panel shows orthotopic mice injected with OVTOKO control and OVTOKO STAT3 overexpression cells. Mouse injected with OVTOKO STAT3 OE cells developed a big tumor in 4 weeks post inoculation but no tumor could be seen in the OVTOKO control mice. Some of the mice injected with control OVTOKO cells, which were left for 3 months, developed a noticeable tumor; **H:** The weight of the ovarian tumor was significantly higher in the STAT3 OE transfected OV cells transplanted mice when compared to the OV cells transplanted mice.

Fig. 3: HO-3867 targets STAT3 and its associated genes in OCCC cells**. A:** Western blot of proteins extracted from OCCC cells with/without treatment with HO-3867 at 5 or 10μM concentrations of HO-3867. The membrane was blotted for pSTAT3 705 (1st row), pSTAT3 727 (2nd row), total STAT3 (3rd row) and β-actin (4th row) for OVTOKO (left column) and JHOC cells (right column). **B:** quantitative results of pSTAT3 Tyr705 bands by densitometry analysis in HO-3867 treated cells. **C:** HO-3867 inhibit DNA-binding of STAT3, as indicated by ELISA assay results. **D:** Western blot for genes associated with STAT3 upstream. The membrane was blotted for JAK1 (1st row), TYK2 (2nd row), ERK 1/2 (3rd row), CDK5 (4th row) for OVTOKO (left column) and JHOC cells (right column). **E:** Western blot for genes associated with STAT3 downstream. The membrane was blotted for MCL1 (1st row), BCl2 (2nd row), cyclin D2 (3rd row) and c-myc (4th row) for OVTOKO (left column) and JHOC cells (right column). **F:** RT-qPCR of OVTOKO cells post treatment with HO-3867, with primers specific for STAT3 and regulatory genes- JAK1, BCl2, c-myc and cyclin D1. **G:** ubiquitination status of the OVTOKO (left panel) and JHOC (right panel) cells post treatment with HO-3867. Increased degradation in both OVTOKO and JHOC cells post treatment for both the concentrations.

Fig. 4: The survival-inhibitory effect of HO-3867 on OCCC. **A:** The cell number was counted at days 1, & 2 after HO-3867 incubated. A dosage- dependent inhibition of cell survival is shown.

Cell viability assay in HO-3867 treated OCCC. OCCC were seeded on a 6 well plate, and incubated with each concentration of HO-3867 up to 2days. Activation of the caspase cascade pathway by HO-3867. **B:** Western blot of proteins extracted from OCCC cells with/without treatment with HO-3867 at 5 or 10μM concentrations of HO-3867. The membrane was blotted for PARP (1st row), cleaved caspase 3 (2nd row), cleaved caspase 7 (3rd row) and β-actin (4th row) for OVTOKO (left column) and JHOC cells (right column). **C:** Cytograms obtained from Annexin V assays of HO-3867 (10 μM) -treated OVTOKO (bottom row) and JHOC (top row) cells. Each cytogram consists of data showing live cells (PI and FITC negative) bottom left; early apoptotic population (FITC positive) bottom right; mid-late stage apoptosis (PI and FITC positive) top left; necrotic/end stage apoptotic cells (PI positive, FITC negative) top right. Left column: control untreated cells; Right column: HO-3867-treated cells. The live cell population is indicated for each sample and is representative of typical data obtained. **D:** Data shown are representative of triplicate experiments and the numbers refer to the mean (and standard deviation) live (PI and FITC negative) populations (expressed as a percentage of the untreated controls). **E:** STAT3 OE transfected OCC cells are resistant to HO-3867 10uM treatment. **F:** The STAT3 plasmid gene was transiently transfected into OV cells. At 24 hours after the transfection of the STAT3 gene, HO-3867 10uM was added into the culture medium of the cells. The untransfected cells with vehicle (DMSO) alone, the untransfected cells with the HO-3867exposure. The STAT3 gene–transfected OV cells inhibit the HO-3867-induced cleavages of caspase-3, -7 and PARP. **G & H:** Cellular absorption of HO-3867 10uM using electron paramagnetic resonance (EPR) spectrometry to quantify the intracellular content of HO-3867 in various time points in OVTOKO and ES2 OCCC cell lines. Results showed that HO-3867 rapidly entered the cells within the 1st hour of treatment period.

Fig. 5: Inhibition of angiogenesis by HO-3867 correlates with inhibition of STAT3 phosphorylation. **A:** Suppression of angiogenesis formation by HO-3867 in HUVEC cells after VEGF (10 ng/ml) stimulation. HUVEC cells were grown and stimulated with VEGF (10 ng/ml) for 10 min and treated with HO-3867 for 6 and 12hrs. **B**: 3D-Angiogenesis Assay (PromoCell) which demonstrates the entire angiogenesis process in vitro – proteolytic activity, migration, proliferation, and lumen formation. The number and length of the sprouts demonstrates the anti-

angiogenicity of HO-3867 in comparison to the control group. HO-3867 inhibits HUVEC tube formation. HUVECs were grown in M200, and incubated with PBS or VEGF (10 ng/ml) for 18–20 hr in the absence or presence of HO-3867 (10μM). Tube formation was quantified (bottom right panel) as described in Materials and Methods. **C:** Invasion was determined using Matrigel coated membranes (photomicrographs show representative fields). Each data set represents the mean SE for at least 3 independent experiments. **D:** The STAT3 inhibitor, HO-3867, induces cytoskeletal changes in cultured HUVEC cells. HUVEC cells cultured in 4-well chamber slides were treated with PBS, VEGF (10 ng/mL) alone, VEGF with DMSO or HO-3867 (10 μM) for 18 hrs. The cultures were then probed using anti-β tubulin primary antibodies (green), and F-actin was stained using phalloidin (red). White arrows highlight F-actin localization at the leading edge, while white arrowheads indicate the curling of microtubules at the cell periphery. 2006magnification. Slice depth = 1 mm. Scale bar = 20 mm. Inset 400magnification.

References:

1. Gounaris I, Brenton JD. Molecular pathogenesis of ovarian clear cell carcinoma. Future Oncol. 2015;11: 1389-1405.
2. Anglesio MS, Carey MS, Kobel M, Mackay H, Huntsman DG, Vancouver Ovarian Clear Cell Symposium S. Clear cell carcinoma of the ovary: a report from the first Ovarian Clear Cell Symposium, June 24th, 2010. Gynecol Oncol. 2011;121: 407-415.
3. del Carmen MG, Birrer M, Schorge JO. Clear cell carcinoma of the ovary: a review of the literature. Gynecol Oncol. 2012;126: 481-490.
4. Sugiyama T, Kamura T, Kigawa J, et al. Clinical characteristics of clear cell carcinoma of the ovary: a distinct histologic type with poor prognosis and resistance to platinum-based chemotherapy. Cancer. 2000;88: 2584-2589.
5. Mackay HJ, Brady MF, Oza AM, et al. Prognostic relevance of uncommon ovarian histology in women with stage III/IV epithelial ovarian cancer. Int J Gynecol Cancer. 2010;20: 945-952.
6. Tan DS, Miller RE, Kaye SB. New perspectives on molecular targeted therapy in ovarian clear cell carcinoma. Br J Cancer. 2013;108: 1553-1559.
7. Matsuzaki S, Yoshino K, Ueda Y, et al. Potential targets for ovarian clear cell carcinoma: a review of updates and future perspectives. Cancer Cell Int. 2015;15: 117.
8. Akira S. Roles of STAT3 defined by tissue-specific gene targeting. Oncogene. 2000;19: 2607-2611.
9. Yu H, Lee H, Herrmann A, Buettner R, Jove R. Revisiting STAT3 signalling in cancer: new and unexpected biological functions. Nat Rev Cancer. 2014;14: 736-746.
10. Saini U, Naidu S, ElNaggar AC, et al. Elevated STAT3 expression in ovarian cancer ascites promotes invasion and metastasis: a potential therapeutic target. Oncogene. 2016.
11. Selvendiran K, Bratasz A, Kuppusamy ML, Tazi MF, Rivera BK, Kuppusamy P. Hypoxia induces chemoresistance in ovarian cancer cells by activation of signal transducer and activator of transcription 3. Int J Cancer. 2009;125: 2198-2204.
12. Chandler RL, Damrauer JS, Raab JR, et al. Coexistent ARID1A-PIK3CA mutations promote ovarian clear-cell tumorigenesis through pro-tumorigenic inflammatory cytokine signalling. Nat Commun. 2015;6: 6118.
13. Anglesio MS, George J, Kulbe H, et al. IL6-STAT3-HIF signaling and therapeutic response to the angiogenesis inhibitor sunitinib in ovarian clear cell cancer. Clin Cancer Res. 2011;17: 2538-2548.
14. Rath KS, Naidu SK, Lata P, et al. HO-3867, a safe STAT3 inhibitor, is selectively cytotoxic to ovarian cancer. Cancer Res. 2014;74: 2316-2327.
15. Selvendiran K, Tong L, Bratasz A, et al. Anticancer efficacy of a difluorodiarylidenyl piperidone (HO-3867) in human ovarian cancer cells and tumor xenografts. Mol Cancer Ther. 2010;9: 1169-1179.
16. Selvendiran K, Ahmed S, Dayton A, et al. Safe and targeted anticancer efficacy of a novel class of antioxidant-conjugated difluorodiarylidenyl piperidones: differential cytotoxicity in healthy and cancer cells. Free Radic Biol Med. 2010;48: 1228-1235.
17. Selvendiran K, Tong L, Vishwanath S, et al. EF24 induces G2/M arrest and apoptosis in cisplatin-resistant human ovarian cancer cells by increasing PTEN expression. J Biol Chem. 2007;282: 28609-28618.
18. Chacko SM, Ahmed S, Selvendiran K, Kuppusamy ML, Khan M, Kuppusamy P. Hypoxic preconditioning induces the expression of prosurvival and proangiogenic markers in mesenchymal stem cells. Am J Physiol Cell Physiol. 2010;299: C1562-1570.

19. Selvendiran K, Koga H, Ueno T, et al. Luteolin promotes degradation in signal transducer and activator of transcription 3 in human hepatoma cells: an implication for the antitumor potential of flavonoids. Cancer Res. 2006;66: 4826-4834.
20. Dayton A, Selvendiran K, Kuppusamy ML, et al. Cellular uptake, retention and bioabsorption of HO-3867, a fluorinated curcumin analog with potential antitumor properties. Cancer Biol Ther. 2010;10: 1027-1032.
21. Yoo JY, Hurwitz BS, Bolyard C, et al. Bortezomib-induced unfolded protein response increases oncolytic HSV-1 replication resulting in synergistic antitumor effects. Clin Cancer Res. 2014;20: 3787-3798.
22. Yu H, Jove R. The STATs of cancer--new molecular targets come of age. Nat Rev Cancer. 2004;4: 97-105.
23. Bhattacharyya S, Yu H, Mim C, Matouschek A. Regulated protein turnover: snapshots of the proteasome in action. Nat Rev Mol Cell Biol. 2014;15: 122-133.
24. Ristic G, Tsou WL, Todi SV. An optimal ubiquitin-proteasome pathway in the nervous system: the role of deubiquitinating enzymes. Front Mol Neurosci. 2014;7: 72.
25. Weissman AM, Shabek N, Ciechanover A. The predator becomes the prey: regulating the ubiquitin system by ubiquitylation and degradation. Nat Rev Mol Cell Biol. 2011;12: 605-620.
26. Teng TS, Lin B, Manser E, Ng DC, Cao X. Stat3 promotes directional cell migration by regulating Rac1 activity via its activator betaPIX. J Cell Sci. 2009;122: 4150-4159.
27. Bid HK, Roberts RD, Cam M, et al. DeltaNp63 promotes pediatric neuroblastoma and osteosarcoma by regulating tumor angiogenesis. Cancer Res. 2014;74: 320-329.
28. Mabuchi S, Sugiyama T, Kimura T. Clear cell carcinoma of the ovary: molecular insights and future therapeutic perspectives. J Gynecol Oncol. 2016;27: e31.
29. Hisamatsu T, Mabuchi S, Matsumoto Y, et al. Potential role of mTORC2 as a therapeutic target in clear cell carcinoma of the ovary. Mol Cancer Ther. 2013;12: 1367-1377.
30. Rosen DG, Mercado-Uribe I, Yang G, et al. The role of constitutively active signal transducer and activator of transcription 3 in ovarian tumorigenesis and prognosis. Cancer. 2006;107: 2730-2740.
31. McCann GA, Naidu S, Rath KS, et al. Targeting constitutively-activated STAT3 in hypoxic ovarian cancer, using a novel STAT3 inhibitor. Oncoscience. 2014;1: 216-228.
32. Guo C, Yang G, Khun K, et al. Activation of Stat3 in renal tumors. Am J Transl Res. 2009;1: 283-290.
33. Qin J, Yang B, Xu BQ, et al. Concurrent CD44s and STAT3 expression in human clear cell renal cellular carcinoma and its impact on survival. Int J Clin Exp Pathol. 2014;7: 3235-3244.
34. ElNaggar AC, Saini U, Naidu S, et al. Anticancer potential of diarylidenyl piperidone derivatives, HO-4200 and H-4318, in cisplatin resistant primary ovarian cancer. Cancer Biol Ther. 2016: 0.
35. Mabuchi S, Kawase C, Altomare DA, et al. Vascular endothelial growth factor is a promising therapeutic target for the treatment of clear cell carcinoma of the ovary. Mol Cancer Ther. 2010;9: 2411-2422.
36. Jin Y, Li Y, Pan L. The target therapy of ovarian clear cell carcinoma. Onco Targets Ther. 2014;7: 1647-1652.
37. Tsuchiya A, Sakamoto M, Yasuda J, et al. Expression profiling in ovarian clear cell carcinoma: identification of hepatocyte nuclear factor-1 beta as a molecular marker and a possible molecular target for therapy of ovarian clear cell carcinoma. Am J Pathol. 2003;163: 2503-2512.

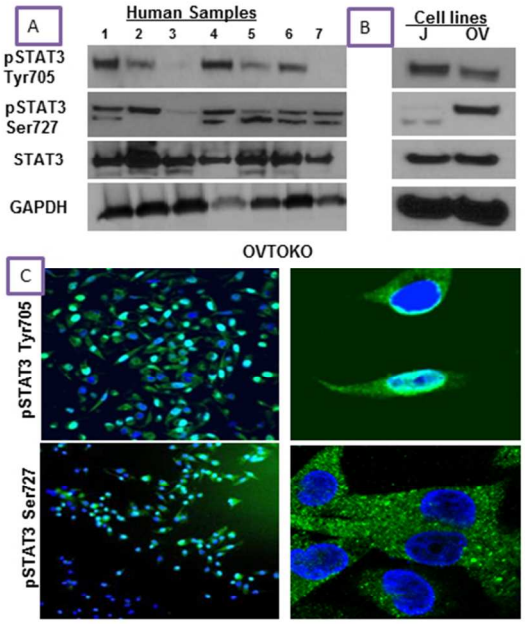

Figure 1

190x254mm (96 x 96 DPI)

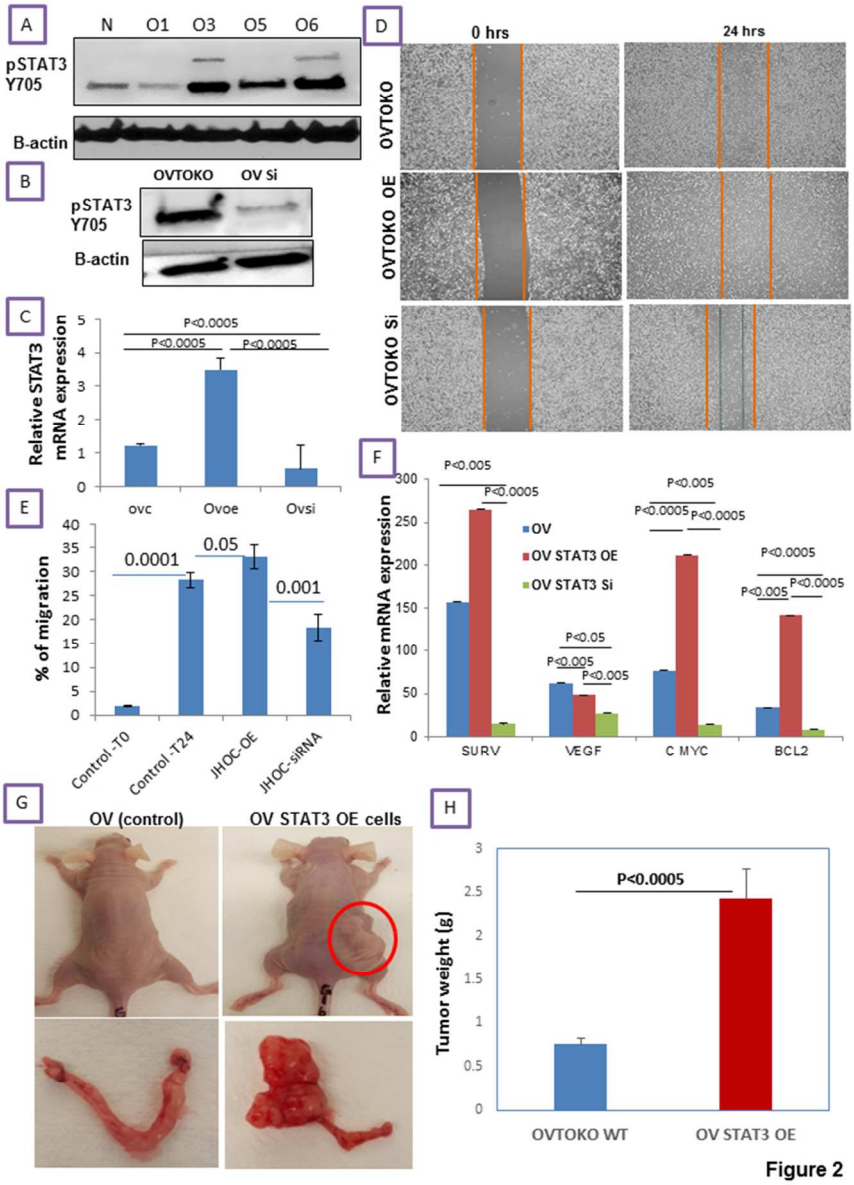

Figure 2

Fig.2

190x254mm (96 x 96 DPI)

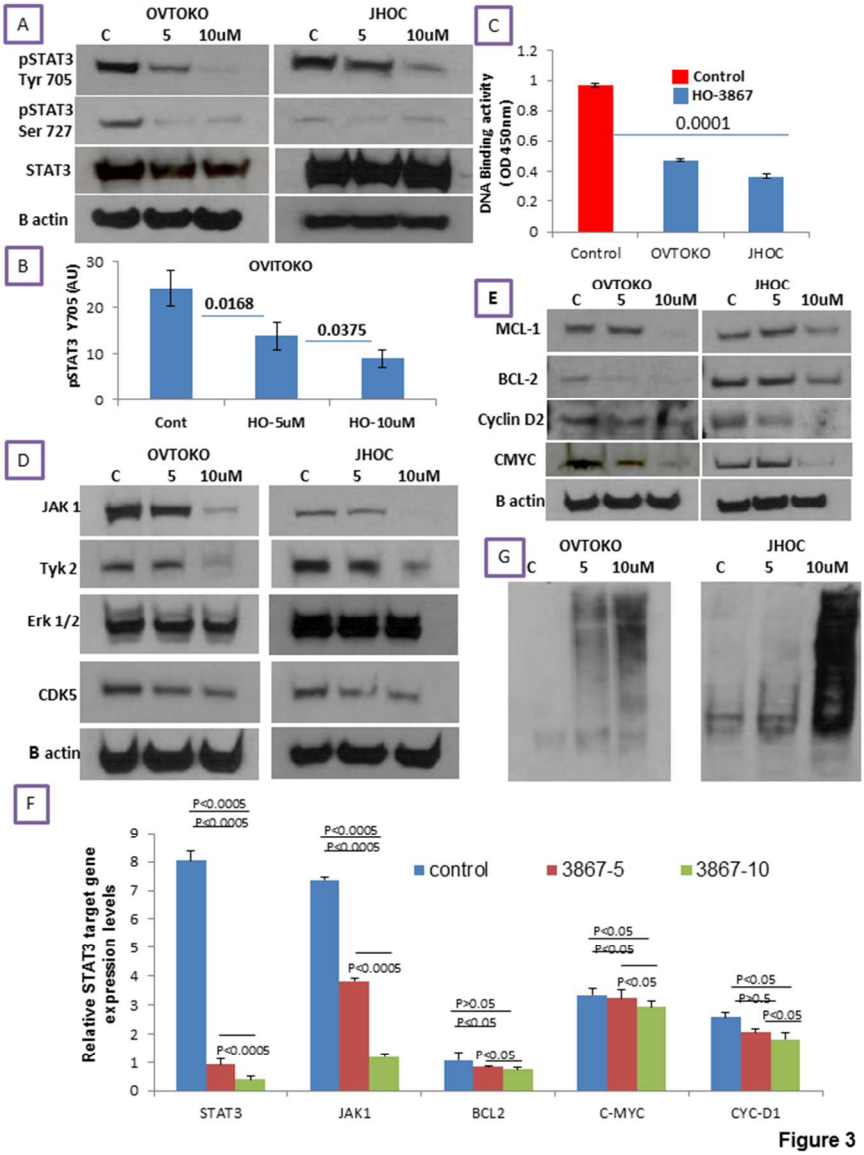

Figure 3

Fig.3

190x254mm (96 x 96 DPI)

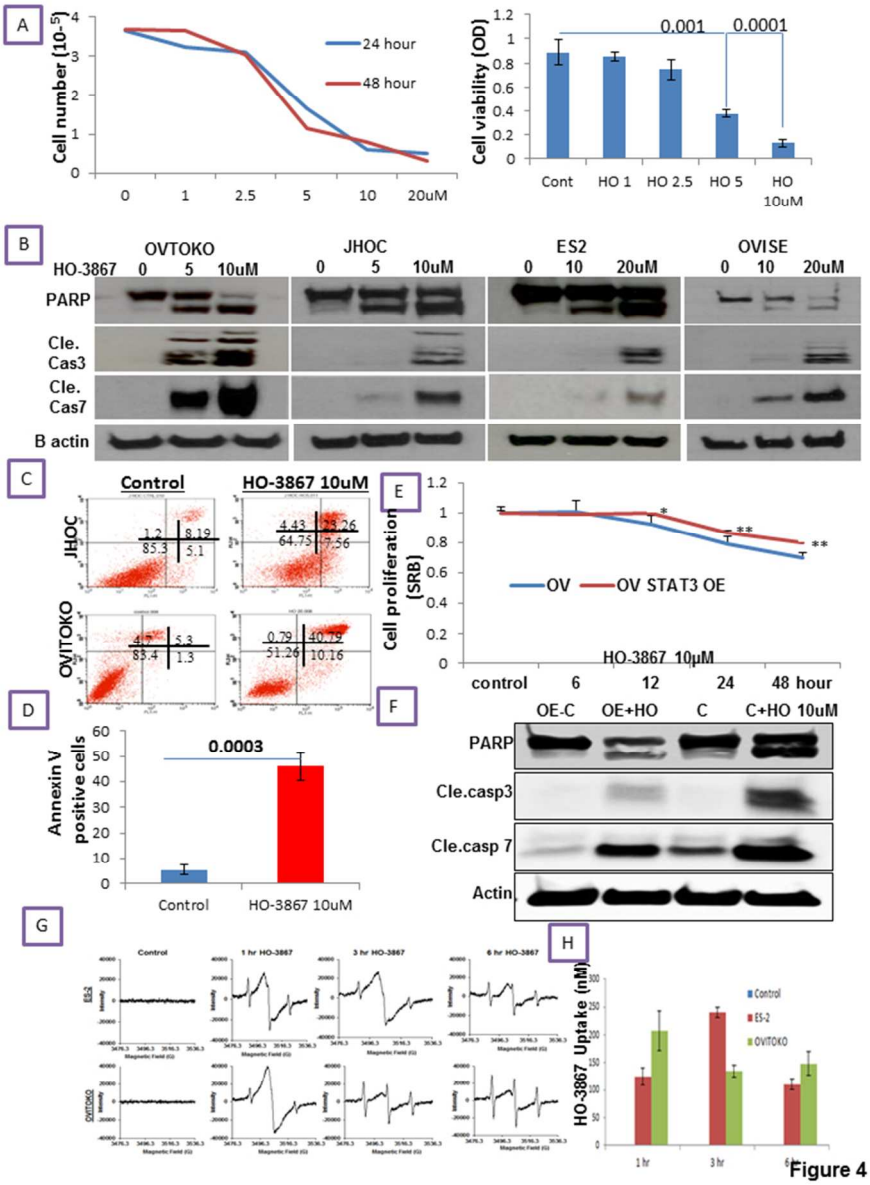

Figure 4

Fig.4

190x254mm (96 x 96 DPI)

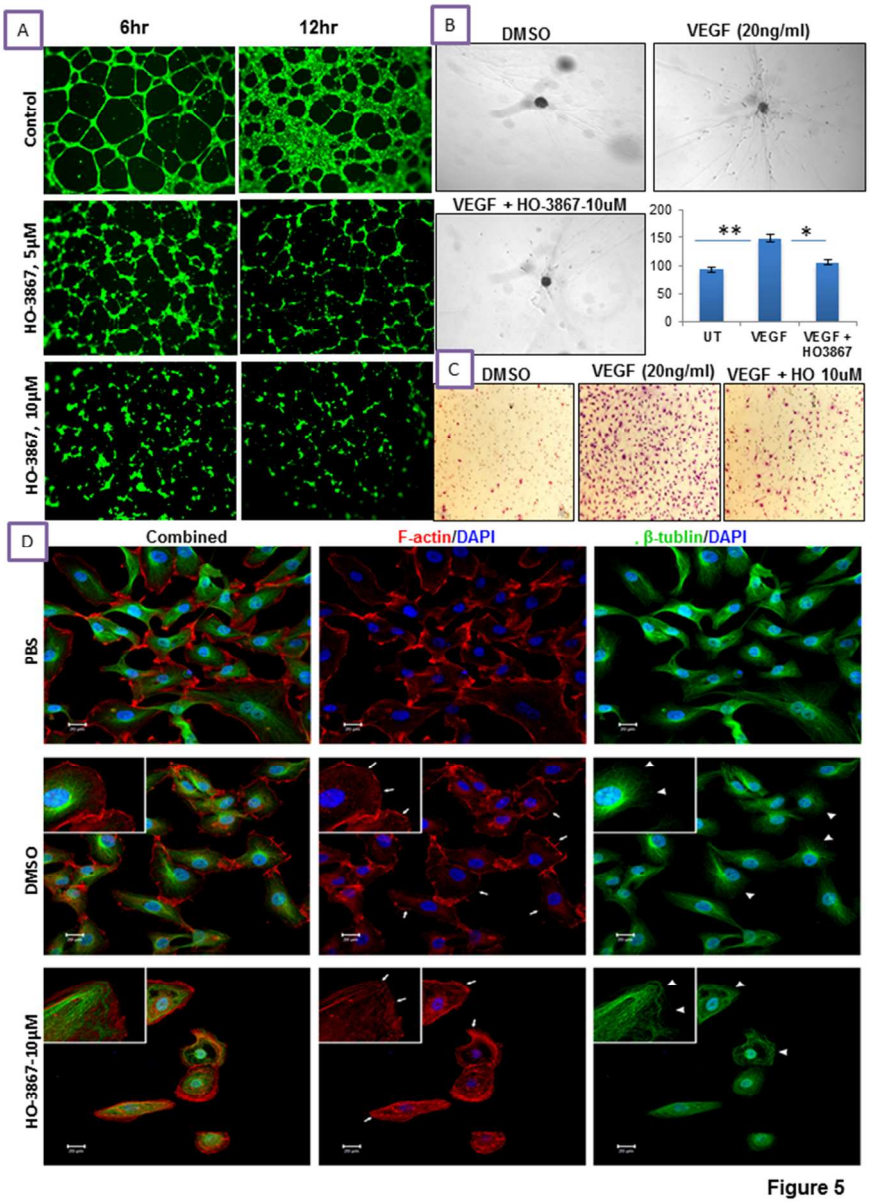

Figure 5

Fig.5

190x254mm (96 x 96 DPI)